

Experimental investigation of the interaction of the wave fields of Mössbauer and x-ray radiations with a crystal under the Bragg diffraction conditions

G. V. Smirnov and A. I. Chumakov

I. V. Kurchatov Institute of Atomic Energy, Moscow

(Submitted 30 April 1985)

Zh. Eksp. Teor. Fiz. **89**, 1169–1180 (October 1985)

The same ^{57}Fe crystal was used in the determination of the angular dependences of the reflection and electron emission in the case of diffraction of Mössbauer radiation (resonant nuclear scattering) and of x rays (electron Rayleigh scattering). The results were analyzed from the point of view of the difference between the behavior of an electromagnetic wave field in a crystal in these two cases. Suppression of a nuclear reaction was deduced for the first time from the yield of the products (conversion electrons) of the inelastic interaction channel. The Mössbauer spectra of the yield of conversion electrons were determined in the exact Bragg position and far from it. The degree of suppression of the electron yield was found for various nuclear transitions.

1. INTRODUCTION

The discovery of the Mössbauer effect has given rise to a new branch of theoretical and experimental optics. It covers a wide range of coherent interaction phenomena between resonant gamma radiation and the nuclei in crystal lattices (a brief review is given in Ref. 1). The ability to vary in the same experiment the scattering and absorption powers of a material, as well as its polarization characteristics (particularly under conditions of the hyperfine splitting of the nuclear levels), the absence of a form factor in the nuclear scattering, and many other features of nuclear gamma resonance provide a rich canvas for the unique features of the coherent interaction between resonant gamma radiation and crystals.

The characteristic features of the scattering of electromagnetic radiation are manifested particularly in the structure of the wave field which is formed in a crystal under diffraction conditions. At the Mössbauer-radiation wavelength a crystal behaves as a three-dimensional diffraction grating in respect of this radiation. A primary electromagnetic wave incident on a crystal excites intra-atomic electron and nuclear oscillating currents which in turn are sources of secondary electromagnetic radiation. In accordance with the Ewald concept, the structure of the wave field which appears in a sufficiently thick single crystal is dictated by the conditions of the dynamically matched interaction between the field and elementary currents. When diffraction takes place, the field becomes a standing electromagnetic wave representing a superposition of several coherent waves excited in a crystal.

Under these conditions the interaction between radiation and matter becomes very unusual. A striking example of the unusual features is the ability to suppress inelastic interaction channels, such as the photoelectric absorption of x rays (Borrmann effect) or conversion of resonant gamma radiation into electrons (Kagan-Afanas'ev effect or suppression of nuclear reactions).²

We shall describe an experimental investigation of the formation of a wave field in a crystal under the Bragg diffraction conditions, the localization of the field relative to the

crystal lattice, and the interaction of the field with atomic centers. This was done by observing the yield of the products of the inelastic channel in the form of conversion electrons or photoelectrons, because the yield of these particles depended directly on the amplitude and polarization of the wave field at the points of location of the atomic centers.

Detection of the conversion electrons is an effective method for investigating the configuration of an electromagnetic wave field and its interaction with the nuclear and electron systems of a crystal. The principal difference between the resonant nuclear and electron Rayleigh interactions of radiation with a crystal is as follows: the configuration of the wave fields formed when a field is scattered by nuclei (Mössbauer radiation) is very different from the corresponding configuration for the scattering of a field by the electron shells of atoms (x rays).

Our aim was to use the same crystal for a comparative investigation of the wave fields formed in the case of the Bragg diffraction of Mössbauer and x-ray radiations.

2. APPARATUS AND EXPERIMENTAL CONDITIONS

A method for detection of electrons under conditions of diffraction of Mössbauer radiation was developed. A proportional gas-filled continuous-flow electron counter was specially constructed for the operation under the conditions of diffraction of gamma rays. The main differences from traditional gas-filled proportional electron counters (such as those used in Mössbauer conversion spectroscopy) were as follows. Firstly, a high (for this class of electron detector) energy resolution amounting to 16–20% made it possible to analyze the energy spectrum of the emerging electrons and thus scan the crystal with depth. Secondly, the relatively low noise background (2×10^{-3} electrons per second) made it possible to carry out measurements using extremely low radiation fluxes. A detailed description of the construction of a counter and its working characteristics can be found in Ref. 3.

The experimental arrangement is shown in Fig. 1a. Resonant nuclear radiation from a ^{57}Co source in a chromium

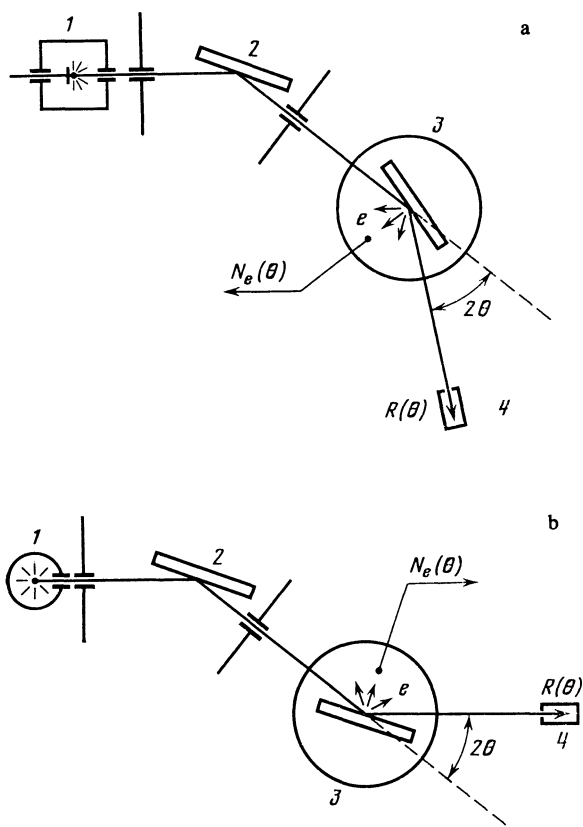


FIG. 1. Schematic diagram of the apparatus used to study Mössbauer (a) and x-ray (b) radiations: 1) a ^{57}Co source of Mössbauer radiation on a vibrator rod (case a) or an x-ray tube, as source (case b); 2) monochromator and collimator (Ge {220}); 3) proportional counter of electrons containing the investigated ^{57}Fe {110} crystal inside it; 4) scintillation detector for the reflected beam. a) $E_\gamma = 14.4$ keV and $\Delta m = 0$; b) $E_{x-r} = 8.05$ keV.

matrix (activity 200 mCi) was first made monochromatic and was collimated by reflection from a perfect germanium crystal. A beam collimate down to $7''$ reached a ^{57}Fe crystal located inside the proportional counter and used to investigate the Bragg reflection from {110} planes. The radiation reflected from the crystal was recorded by a scintillation detector. Voltage pulses from the proportional counter and from the scintillation detector were first amplified and then applied to two NTA-512 multichannel pulse analyzers. A control system for the vibrator which set in motion the Mössbauer source made it possible to operate in the constant-acceleration and constant-velocity regimes. The angular dependences of the electron yield and of the reflection of gamma photons were determined in the constant-velocity regime. A resonant nuclear transition accompanied by a change in a magnetic quantum number $\Delta m = 0(1/2 \leftrightarrow 1/2)$ was studied.

The main experimental difficulty was that the rate of counting of the conversion electrons was extremely low. The useful count was of the order of 0.01 electrons/sec. Consequently, it was necessary to satisfy stringent requirements in respect of the background in the apparatus, angular stability of the goniometer, and reliability of the whole apparatus.

Several lead screens, selection of the optimal low anode voltage (1260 V for an anode wire diameter 20μ), hermetic sealing of high-voltage connectors and units were used to reduce the level to $(2-3) \times 10^{-3}$ electrons/sec. A very simple heat screen (the goniometer was placed under a heat screen made of Plexiglas) ensured an acceptable stability of the angular position of a crystal which did not drift by more than $1-2''$ in 24 h. During the experiment the ^{57}Fe crystal was rocked 21 times about the Bragg position. The angular interval of $2'$ was scanned in 36 h. The Bragg reflection maxima were determined sufficiently accurately in one pass, so that in the course of addition of the results the angular dependences of the reflection could be made to coincide with the positions of these peaks. The angular dependences of the electrons emission were added after combining them at the same relative positions that were deduced from the corresponding reflectivity dependences.

The apparatus used to study the diffraction of x rays is shown in Fig. 1b. Instead of a source, there was an x-ray tube with a copper anticathode. The CuK_α radiation was collimated with an asymmetrically cut monochromator in the form of a Ge {220} crystal with asymmetry index $\beta = 0.067$. the angular divergence of the beam after reflection by the monochromator was approximately $3''$, which was much less than the angular widths of the measured dependences. Consequently we were able to determine the almost intrinsic angular characteristics of the reflection and photoemission. A contribution of the dispersion to the broadening of the curves was small, i.e., use was made of the antidisersion geometry of reflection, and the Bragg angles of two crystals were practically identical. The dispersion broadening in the Mössbauer spectrum was negligible in view of the high monochromaticity of the radiation. Therefore, it seemed desirable to use dispersive reflection geometry, which enabled us to take the detectors out of the primary beam and thus reduce significantly the background.

3. INVESTIGATED ^{57}Fe CRYSTAL

Our crystal was enriched to 85% with the ^{57}Fe isotope and it was in the form of a disk 2.5–3 mm in diameter and 60μ thick. The large surface of the disk was parallel to the {110} crystallographic planes. The "perfection" of the crystal was confirmed in earlier experiments⁴ in which it was used. A homogeneous magnetization of a crystal was achieved by the application of a constant magnetic field of about 40 G intensity. The subsequent interpretation of the experimental results and a theoretical analysis of the situation could be simplified by selecting the direction of the magnetic field vector at right-angles to the scattering plane (\mathbf{k}' , \mathbf{k}). The crystal was oriented in such a way that the easy-magnetization [100] crystallographic axis coincided with the magnetic field vector. The polarization factors in the expressions for the nuclear amplitudes could then be such that the π -polarized component of the radiation was scattered only as a result of resonant transitions $1/2 \leftrightarrow 1/2$ and $-1/2 \leftrightarrow -1/2$, whereas in the case of the σ -polarized components of the radiation the scattering was due to $3/2 \leftrightarrow 1/2$, $-3/2 \leftrightarrow -1/2$, $1/2 \leftrightarrow -1/2$, and $-1/2 \leftrightarrow 1/2$ transitions.

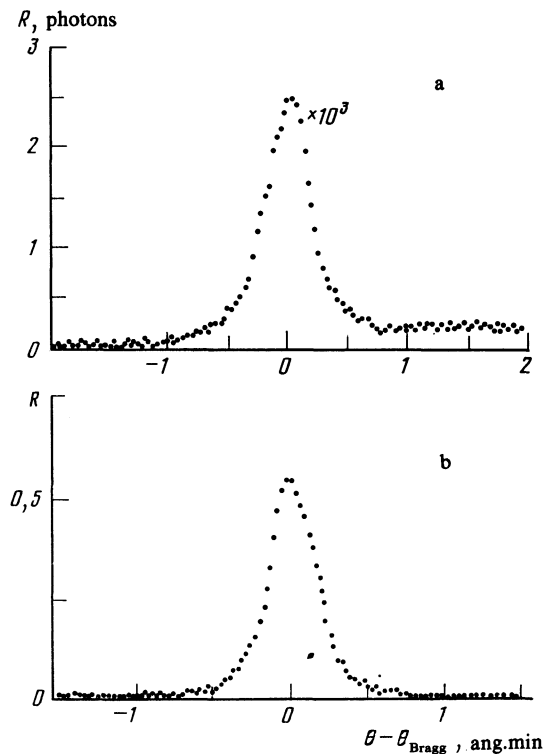


FIG. 2. Angular dependences of the reflection $R(\theta)$ of Mössbauer (a) and x-ray (b) radiations.

4. RESULTS AND DISCUSSION

The angular characteristics of the diffraction process were determined using the system shown in Fig. 1. Figure 2 gives the angular dependences of the Bragg reflection of the resonant gamma rays (a) and of the x rays (b) from a $\{110\}$ plane of a ^{57}Fe single crystal. Figure 3b shows the corresponding angular dependences of the electron emission.

In the case of the resonant nuclear scattering of gamma photons the diffraction pattern is a function not only of the angle of incidence of gamma radiation on a crystal, but also of the energy of the photons relative to the resonance. These two parameters determine the structure of the wave field in a crystal, the reflectivity of the crystal, and naturally the yield of the products of the interaction between the radiation field and atoms. We ensured that the diffraction pattern was more complete by recording also the Mössbauer spectra of the conversion electrons. Figure 4a shows a spectrum recorded in the case of the Bragg scattering, and Fig. 4b shows a spectrum obtained in the case of the non-Bragg scattering of gamma radiation. In the latter case the radiation was not collimated by a germanium crystal, but was simply made monochromatic by reflection from a mosaic crystal of pyrolytic graphite.

We shall first analyze the pattern of the electron yield obtained as a result of the diffraction of resonant gamma radiation in a crystal (Fig. 3a). The cross section for the resonant absorption of gamma photons by iron nuclei is almost two orders of magnitude higher than the photoemission cross section. Therefore, under the experimental condi-

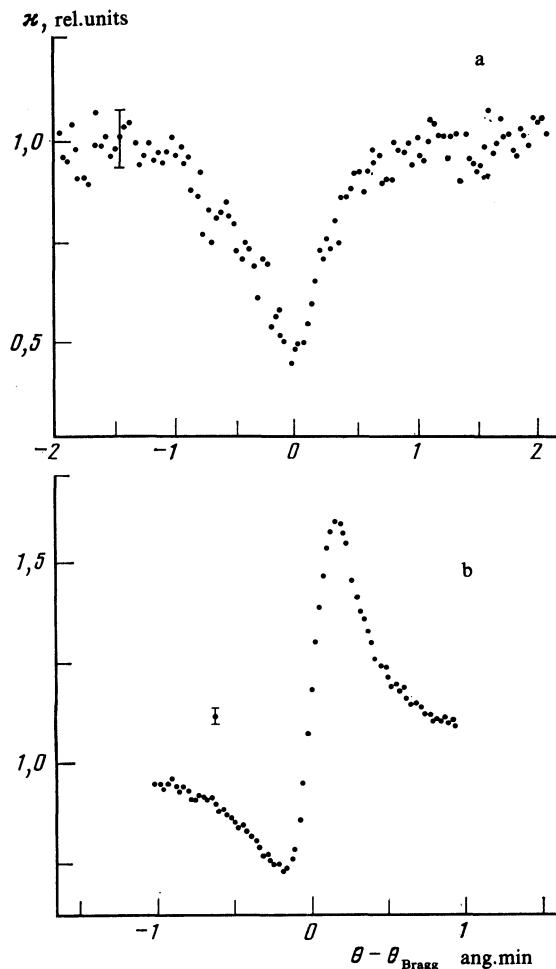


FIG. 3. Angular dependences of electron emission $\kappa(\theta)$ in the case of the diffraction of Mössbauer (a) and x-ray (b) radiations.

tions when the radiation line is tuned exactly to a resonant nuclear transition, the main process of electron creation is internal conversion and, consequently, we can quite justifiably regard the recorded spectrum (Fig. 3a) as primarily the angular dependence of the conversion-electron yield. Some contribution to the total intensity is made also by Auger electrons released from the atoms as a result of changes in the atomic electron shells following the emission of the conversion electrons. However, the Auger electrons are also the products of the resonant excitation of the nuclei.

All the released particles are created in a surface layer of a crystal of thickness governed by the range of the conversion and Auger electrons of energies 7.3 and 5.7 keV in the investigated material. We found that the maximum depth from which particles could leave an iron crystal was approximately 3000 Å. Therefore, the observed pattern represented the interaction of the wave field with matter in just this thin surface layer. It should be pointed out that the thickness of this layer was much less than the depth of penetration of the wave fields into the crystal.

Far from the Bragg angle the wave field represents a wave traveling in a crystal. Consequently, in this range of angles the intensity of electron emission reflects the interac-

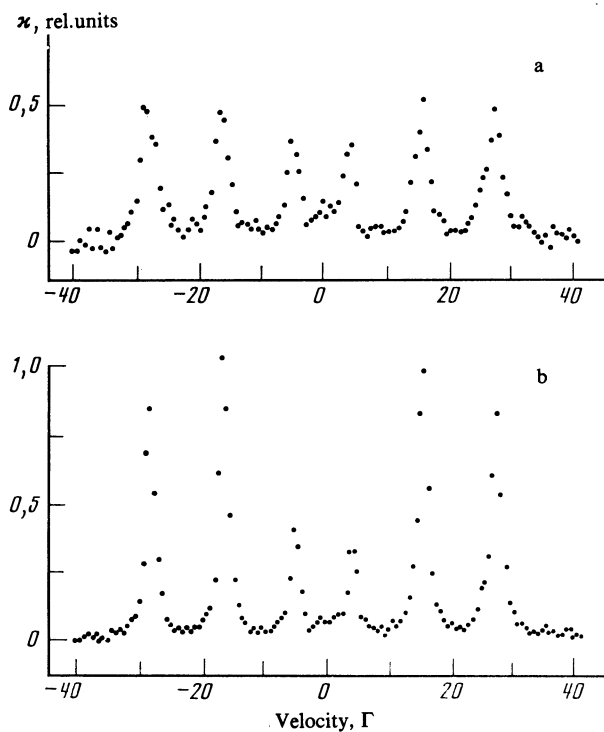


FIG. 4. Mössbauer spectra of the electron yield recorded in the exact Bragg position (a) and far from this position (b).

tion of a traveling radiation wave with atoms on the surface. As we approach the Bragg angle a diffracted wave grows in a crystal and the wave field assumes a complex configuration. We shall not go into details of the structure of the resultant field, but on the basis of the fall of the conversion electron yield we can say that the resonant excitation of the nuclei by the radiation field established in a crystal decreases strongly. Therefore, the result obtained is direct evidence of the suppression of a nuclear reaction in a crystal in the vicinity of the Bragg angle. In addition to the anomalous transition of resonant gamma rays by a crystal⁴ and the anomalously high reflection coefficient of a crystal,¹ the fall of the conversion electron yield (observed for the first time under the diffraction conditions) provide a direct proof of the occurrence of nuclear reaction suppression.

Such suppression occurs because the amplitudes of the excitation of nuclei by the electromagnetic radiation field decrease to zero. Using the structure of the excitation amplitude, which in the case of a magnetic dipole transition is proportional to the scalar product $\mathbf{h} \cdot \boldsymbol{\mu}$, where \mathbf{h} is the magnetic component of the total wave field in the nucleus and $\boldsymbol{\mu}$ is the magnetic moment related to the oscillating electric current excited in the nucleus, we can draw conclusions on the amplitude and polarization of the wave field at the points occupied by nuclei. For a given magnetization of a crystal, the investigated nuclear $1/2 \leftrightarrow 1/2$ resonant transition can be excited only by the π -polarized component of the electromagnetic field, i.e., by that component for which the magnetic vector \mathbf{h} oscillates at right-angles to the scattering plane. The suppression of a nuclear reaction in this case shows that the amplitude of the oscillations at the points of

location of the nuclei is quenched or reduced significantly compared with the amplitude of a traveling wave.

We shall now turn to a comparative analysis of the angular dependences of the reflected magnetic rays (Figs. 2a and 2b) and of the angular dependences of electron emission (Figs. 3a and 3b) in the scattering of Mössbauer and x-ray radiations near the Bragg angle of a crystal.

The reflection curves show no qualitative difference: in both cases there is a reflection intensity maximum approximately in the same angular interval in the vicinity of the Bragg angle. Under the same conditions the observed electron emission pattern is basically different for each of the investigated cases. The angular dependences of the conversion electron yield (Fig. 3a) is quite different from the angular dependence of the emitted photoelectrons (Fig. 3b). In the Mössbauer radiation case there is a dip of almost symmetric shape relative to the Bragg angle. However, the yield of photoelectrons in the diffraction of x rays decreases to its minimum value on approach to the Bragg angle and then rises linearly reaching a maximum which is followed again by a return to the unity level.

The experimental angular dependence of the photoelectron yield also reflects directly the behavior of the electromagnetic field in a crystal in the vicinity of the Bragg angle. It is known that photoelectric absorption is proportional to the intensity of the electromagnetic field inside an electron shell. Therefore, change in the photoelectron yield is direct evidence of a change in the field intensity at the points of location of the atoms.

It follows from the angular dependence of the photoemission that the intensity of the wave electric field established at the atomic positions because of diffraction may be considerably greater and considerably less than the intensity of a traveling wave. In other words, the interaction of x rays with matter may be weakened or enhanced, in contrast to the interaction pattern observed in the case of resonant scattering of Mössbauer radiation when only a weakening of the interaction can take place.

Such very different behavior of the wave fields in a crystal is due to qualitative differences between the nature of the scattering of the radiation by atoms in the investigated cases. Depending on whether the scattering is resonant or nonresonant, we can expect characteristic phase relationships between the primary and secondary electromagnetic waves in each of these cases. In the final analysis it is these relationships that govern the structure of an electromagnetic field established in a crystal.

For a quantitative description of the wave field structure in a crystal we shall use the dynamic theory of Kagan and Afanas'ev, which includes both types of scattering of electromagnetic waves: resonant by the nuclei and nonresonant by the electrons.⁵

We shall write down the expression for the amplitude of the wave field inside a planar crystal near its surface. Under the experimental conditions, i.e., in the case of the Bragg diffraction by one system of planes, we can see that the theory gives the following expression for the amplitude of the electric field in a crystal when this crystal occupies a symmetric position and in the case when the sample can be de-

scribed approximately as having a large thickness:

$$\mathbf{E}(\mathbf{r}) = \exp(i\mathbf{\kappa}\mathbf{r}) \exp(i\mathbf{\kappa}\varepsilon_0^{(2)} l) \{e_0 E_0 + e_1 E_1 \exp(i\mathbf{K}\mathbf{r})\}, \quad (1)$$

where \mathbf{r} is the coordinate of the point of observation; $\mathbf{\kappa}$ is the wave vector of a plane wave incident on a crystal; $\varepsilon_0^{(1,2)}$ are small complex quantities representing deviation of the refractive index from unity; l is the depth of the point of observation in a crystal along the vector $\mathbf{\kappa}$; $e_{0,1}$ are the orthogonal unit vectors in the direction of the electric component of the wave field for the refracted and diffracted waves in a crystal, respectively; \mathbf{K} is the reflection vector; $E_{0,1}$ are the scalar amplitudes of the waves:

$$E_0 = E, \quad E_1 = E \tilde{g}_{10} / (2\varepsilon_0^{(4)} - \tilde{g}_{00}), \quad (2)$$

where E is the scalar amplitude of the incident wave and \tilde{g}_{00} and \tilde{g}_{10} are the coefficients in the dynamic equations, which can be represented by a sum of the nuclear and electron parts, for example, $\tilde{g}_{00} = g_{00} + \chi_{00}$, where each of the terms is related in a specific manner to the complex amplitudes of the coherent scattering of radiation by the nuclei and electrons in a unit cell of a crystal. Under the experimental conditions the complex corrections to the refractive index

$$\varepsilon_0^{(1,2)} = 1/4 \{ \alpha \mp [(2\tilde{g}_{00} - \alpha)^2 - 4\tilde{g}_{00}\tilde{g}_{10}]^{1/2} \}; \quad (3)$$

here, $\alpha = -2\Delta\theta \sin 2$ is the angular deviation of the vector $\mathbf{\kappa}$ from the exact Bragg direction. Far from the Bragg position of a crystal we have $\alpha \gg |\tilde{g}|$, so that we approximately find that $\varepsilon_0^{(1)} \approx \alpha/2$ and $\varepsilon_0^{(2)} \approx \tilde{g}_{00}/2$, and only one refracted wave traveling in a crystal remains in the solution for the field (1).

On approach to the angular range of the Bragg reflection, where $\alpha \sim |\tilde{g}|$, the amplitude E_1 in Eq. (2) begins to rise and a second wave, which contributes to the total field, grows in a crystal. We shall find the field formed as a result of interference between two coherent waves at the points of location of the nuclei and identify the angular dependence of the field amplitude. We shall consider two approximate cases: a) $\tilde{g}_{00} = \tilde{g}_{10} = ig_r$, where i is an imaginary unity, $g_r = \mu_r / \lambda$, and μ_r is the value of the linear absorption coefficient at the resonance (this is the approximation of a pure nuclear interaction); b) $\tilde{g}_{00} = \tilde{g}_{10} = \chi_0$, where $\chi_0 = 2 \operatorname{Re}(n - 1)$ and n is the refractive index of a crystal outside the resonance region; in this case we are dealing with the approximation of a purely electron angular scattering of a wave and we are ignoring the photoemission [i.e., in the case under discussion we have $\operatorname{Re}(n - 1) \gg \operatorname{Im}(n)$].

Allowing for a) and expanding in terms of a small parameter α/g_r , we find that near the Bragg angle

$$\varepsilon_0^{(1,2)} \approx \frac{1}{4} \left\{ \alpha \mp (2|\alpha|g_r)^{1/2} \left(-\frac{\alpha}{|\alpha|} + i \right) \right\}. \quad (4)$$

Since the amplitude of the nuclear excitation in the case of a magnetic dipole transition is related directly to the magnetic component of the field, we shall seek this component. As pointed out earlier, only the π -polarized component of the radiation participates in the excited $1/2 \leftrightarrow 1/2$ transition for which the angular dependence of the conversion electron yield was determined. It should be noted that Eq. (1) applies

also to the magnetic component of the field. At the points of location of the nuclei it is found that the equality $\exp(i\mathbf{K} \cdot \mathbf{r}) = 1$ is valid in the case of the reflection by a $\{110\}$ face. Bearing in mind that $\mathbf{h}_0^\pi = \mathbf{h}_1^\pi$, we find that the total amplitude of the magnetic field in the atomic planes is given by

$$|\mathbf{H}_a^\pi(\alpha)| \approx H_0 \left(\frac{|\alpha|}{g_r} \right)^{1/2} \exp \left\{ -\frac{1}{4} \kappa l (2|\alpha|g_r)^{1/2} \right\}, \quad (5)$$

where the terms of a small order α/g_r are omitted.

We can similarly obtain an expression for the field amplitude in the space between the atomic planes. Halfway between the planes we have $\exp(i\mathbf{K} \cdot \mathbf{r}) = -1$ and the modulus of the π -polarized component of the magnetic field is

$$|\mathbf{H}_m^\pi(\alpha)| \approx H_0 \left[2 - \left(\frac{|\alpha|}{2g_r} \right)^{1/2} \right] \exp \left\{ -\frac{1}{4} \kappa l (2|\alpha|g_r)^{1/2} \right\}. \quad (6)$$

We thus find that interference between two waves on approach to the Bragg angle creates a wave field in the form of a standing wave which is periodic at right-angles to the scattering atomic planes in a crystal. The amplitude is modulated in such a way that the field seems to be displaced from the absorption centers to the space between the atomic planes. In the limit $\alpha \rightarrow 0$ it is found that nodes of the field form on the planes and antinodes appear between the planes. Naturally, the absorption of the field disappears: the factor in the exponential function [Eqs. (5) and (6)] vanishes. Such a state is reached at the Bragg angle and a deviation in the direction of lower or higher angles reduces the depth of the amplitude modulations until it disappears completely. This behavior of the field is in agreement with the experimentally determined pattern of emission of the conversion electrons (Fig. 3a).

We shall now analyze the case of nonresonant scattering. We now find that because χ_0 is a real number, the whole angular range splits into three characteristic intervals $]-\infty, 0[$, $]0, 4\chi_0[$, and $]4\chi_0, +\infty[$ with different behavior of the field in each of them. Simple transformations yield the following expression for the amplitude of the electric field in the atomic planes on the surface of a crystal in the Bragg reflection region (for the sake of simplicity, we shall consider only the σ -polarized component of the field for which we have $e_0 = e_1$):

$$\begin{aligned} |E_a^\sigma(\alpha)| &= E \left(\frac{|\alpha|}{\chi_0} \right)^{1/2}, \quad \alpha \leq 0, \quad \frac{|\alpha|}{\chi_0} \ll 1, \\ |E_a^\sigma(\alpha)| &= E \left(\frac{\alpha}{\chi_0} \right)^{1/2} \exp \left\{ -\frac{1}{4} \kappa l [\alpha(4\chi_0 - \alpha)]^{1/2} \right\}, \\ 0 &\leq \alpha \leq 4\chi_0, \end{aligned} \quad (7)$$

$$|E_a^\sigma(\alpha)| = E \left[2 - \left(\frac{\alpha}{\chi_0} - 4 \right)^{1/2} \right], \quad 0 \leq \frac{\alpha}{\chi_0} - 4 \ll 1.$$

In the direct vicinity of the Bragg position where $\alpha = 0$, we find that the behavior of the field on the side of the negative and positive angles is very close to that predicted for the resonant scattering case: the sum of the amplitudes of the refracted and diffracted waves vanishes on the atomic planes near the surface. In the interval between 0 and $4\chi_0$ the field amplitude rises continuously as $\alpha^{1/2}$ and reaches twice the

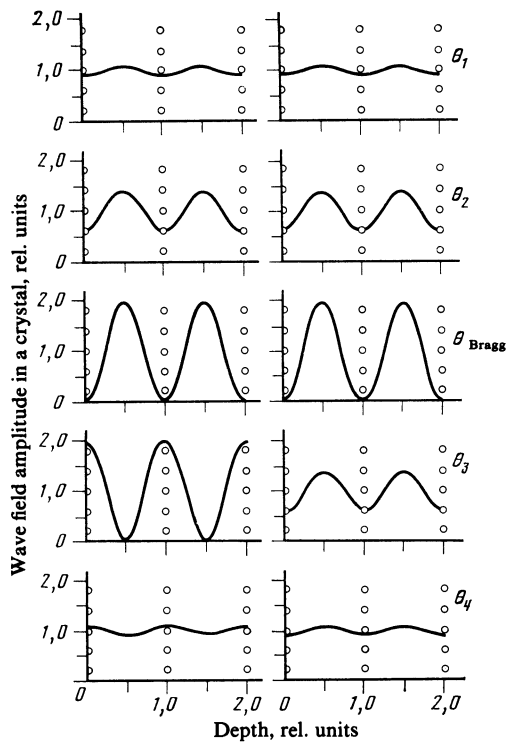


FIG. 5. Schematic representation of the angular dependences of an electromagnetic wave field created in a crystal as a result of diffraction of x rays (on the left) and Mössbauer radiation (on the right). Changes in the amplitude of the wave field at the atomic planes and in the intervals between them are shown for the case when the angle of incidence is gradually increased near the Bragg position ($\theta_1 < \theta_2 < \theta_{\text{Bragg}} < \theta_3 < \theta_4$).

amplitude of the incident wave at the end of the interval. The refractive index then passes through a maximum at the center of the interval. Since this investigation method is limited to very small depths, the exponential factor in Eq. (7) is always close to unity. When the angle exceeds the value $4\chi_0$, the field amplitude begins to fall again. Far from the Bragg angle it again reaches unity.

We can similarly show that between atomic planes the dependence of the field amplitude on the angle is inverted. Therefore, on approach to the Bragg position we find that, in this case as well as in the case of the resonant scattering, a standing wave field with nodes at the atomic planes and antinodes between them is formed. However, unlike the situation in the resonant scattering case, when the contrast of the modulation field decreases symmetrically as we move away from the Bragg angle, we find that in this case within the angular interval $0 < \alpha < 4\chi_0$ the modulated wave field is shifted relative to the crystal lattice along the reflection vector \mathbf{K} and this does not change the modulation contrast. The nodes of the field in the atomic planes change to antinodes. A further increase in the angle reduces the modulation contrast and the traveling wave regime is established. Variation of the contrast of the electromagnetic field amplitude with the angle under conditions of the nuclear and electron scattering is illustrated in Fig. 5. On the whole, the behavior of the field described above is in good agreement with the experimental angular dependence of the photoelectric emission.

Finally, we shall analyze the Mössbauer spectra of the conversion electrons obtained in the presence of traveling and standing waves in a crystal (Figs. 4a and 4b). The intensities of the lines in these spectra are normalized using relationships governing the electron yield at the $\pm 1/2 \leftrightarrow \pm 1/2$ resonance (lines 2 and 5 in the Mössbauer spectrum) obtained for the Bragg and non-Bragg positions of a crystal. It is clear from Fig. 3a that the ratio of the electron yields in these two cases is approximately 1/2. Comparing the line intensities for the other resonances, we find that for lines 1 and 6 the intensity ratio is 1/1.5, whereas for lines 3 and 4 it is approximately 1. In other words, when the $1/2 \leftrightarrow 3/2$ and $-1/2 \leftrightarrow -3/2$ resonances are excited, the transition to the standing wave regime reduces the electron yields, whereas in the case of the $1/2 \leftrightarrow -1/2$ and $-1/2 \leftrightarrow 1/2$ resonances the electron emission is practically unaffected. These results manifest the formation of a wave field under the complex conditions of electron-nuclear scattering of Mössbauer radiation in a crystal.

The above approximation of a purely nuclear resonant scattering is still acceptable for the $1/2 \leftrightarrow 1/2$ resonance, because the electron channel represents simply a small correction ($\sim 10\%$ in the exact resonance case) to the interference process of the formation of a field. In the case of other nuclear resonances this approximation is no longer acceptable. The coherent electron scattering channel begins to play a very important role. The wave phase and polarization relationships become more complex and the relatively simple configurations and forms of behavior of the field discussed above are no longer realized. In the case of ideal pure cases discussed above the scattering amplitude can be either an imaginary quantity (resonant nuclear scattering) or a real quantity (electron Rayleigh scattering). When both these scattering channels are acting simultaneously, each of them has its own amplitude, phase, and polarization, and then the interference between them produces a very complex pattern of the wave fields in a crystal. Figure 6 shows the results of a computer calculation of the angular dependence of the electron emission in the case of electron-nuclear scattering, corresponding to our experimental conditions. As already pointed out, in the case of the $1/2 \rightarrow 1/2$ transition the amplitude of the electron scattering is about 10% of the amplitude

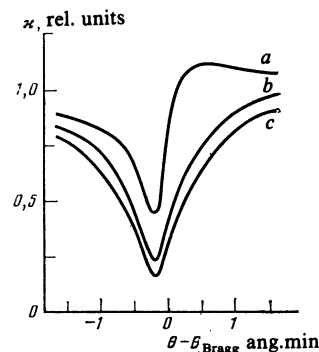


FIG. 6. Calculated angular dependences of the electron emission in the case of $\pm 1/2 \leftrightarrow \mp 1/2$ (a), $\pm 1/2 \leftrightarrow \pm 3/2$ (b), and $\pm 1/2 \leftrightarrow \pm 1/2$ (c) transitions.

of the nuclear scattering. In the case of the resonant scattering involving the $\pm 1/2 \leftrightarrow \pm 3/2$ transitions the contribution of the electron amplitude is again small ($\sim 20\%$), whereas in the case of the $\pm 1/2 \leftrightarrow \mp 1/2$ transitions, it is already $\sim 50\%$. The angular distributions in the case of such mixed electron-nuclear scattering occupy an intermediate position (Figs. 6a and 6b) between the curves representing the pure or ideal cases (Figs. 6c and 3b).

We shall now compare the measured degree of suppression of the electron emission in the Bragg position (Figs. 4a and 4b) with the calculated values of a dip in the angular dependence of the electron yield (Fig. 6). We can see that insufficient perfection of the structure of the surface layers in a crystal reduces the suppression of the electron yield at the exact Bragg position by a factor of about 2 compared with the value calculated for $\pm 1/2 \leftrightarrow \pm 1/2$ (lines 2 and 5) and $\pm 1/2 \leftrightarrow \pm 3/2$ (lines 1 and 6) transitions. On the other hand, in the case of the $\pm 1/2 \leftrightarrow \mp 1/2$ transitions (lines 3 and 4) there is practically no suppression of the yield and the electron yield at such resonances does not change on deviation from the Bragg position (Figs. 4a and 4b) although calculation (Fig. 6a) shows that in the case of an ideal crystal the electron yield should be halved at the exact Bragg position. Therefore, in the case of mixed electron-nuclear scattering the imperfection of the structure of the surface layers of a crystal practically completely cancels out the suppression effect. This sensitivity of the angular dependence of the electron emission to the imperfection of the crystal structure in the case of electron-nuclear scattering is due to the complex nature of the wave field which is created in a crystal. It is clear from Fig. 6a that in the case of the $\pm 1/2 \leftrightarrow \mp 1/2$ transition the angular dependence of the electron emission is characterized by a very steep rise to the right of the Bragg position followed by a maximum at which the electron yield exceeds the yield far from the Bragg angle. Such a strong dependence of the electron emission on the angle of incidence is unavoidably flattened by even a slight angular misorientation of the separate parts of a crystal. Therefore, imperfection of the crystal structure can disturb greatly the suppression of the electron yield in the case of this particular transition. Therefore, a comparison of the calculated (Fig. 6) and experimental (Fig. 4) degrees of suppres-

sion of the electron emission leads to the conclusion that the angular dependence of the electron yield in the case of mixed electron-nuclear scattering is much more sensitive to imperfections of the crystal structure of a sample than in the case of the purely nuclear interaction.

5. CONCLUSIONS

The experimental angular and frequency characteristics of electron emission obtained under the conditions of diffraction of Mössbauer and x-ray radiations reveal an interesting pattern of the behavior of the wave radiation fields in a sample. The different nature of the interactions with different types of radiation of the same crystal gives rise to different configurations of the wave field in a sample. The formation of the wave field, changes in the standing wave contrast, and the motion of a standing field wave relative to the atomic planes of a crystal are all reflected in the angular behavior of the electron emission. Since the electron yield depends directly on the amplitude of the wave field at the atomic centers, this determination gives direct information on the field at the atoms, degree of suppression of the absorption of the field in matter, etc. The high sensitivity of the angular dependence of the electron emission to imperfections of the crystal structure in the surface layers observed under mixed electron-nuclear diffraction conditions provides a means for precise monitoring of the perfection of the crystal surface.

The author regard it as their pleasant duty to thank K. P. Aleshin and M. V. Volkov for their great help in the technical realization of the experiments.

¹H. J. Maurus, U. van Burck, G. V. Smirnov, and R. L. Mössbauer, *J. Phys. C17*, 1991 (1984).

²Yu. Kagan, *Proc. Intern. Conf. on Applications of Mössbauer Effect*, Jaipur, India, 1981, p. 79.

³A. I. Chumakov, A. B. Dubrovin, and G. V. Smirnov, *Nucl. Instrum. Methods Phys. Res.* **216**, 505 (1983).

⁴G. V. Smirnov, N. A. Semioshkina, V. V. Sklyarevskii, S. Kadechkova, and B. Shestak, *Zh. Eksp. Teor. Fiz.* **72**, 340 (1977) [*Sov. Phys. JETP* **45**, 180 (1977)].

⁵Yu. Kagan, A. M. Afanas'ev, and I. P. Perstnev, *Zh. Eksp. Teor. Fiz.* **54**, 1530 (1968) [*Sov. Phys. JETP* **27**, 819 (1968)].

Translated by A. Tybulewicz